Butterfly abundances but not patch occupancy buffered by vegetation heterogeneity during climatic extremes

Natalie E. van Dis[1,2]*, Mirkka M. Jones[1,3], Pekka Niittynen[4], Miska Luoto[5], Jukka Siren[3] &

Marjo Saastamoinen[1,2]

[1]Research Centre for Ecological Change, Organismal and Evolutionary Biology Research Programme, Faculty of Biological and Environmental Sciences, PO BOX 65, 00014 University of Helsinki, Finland

[2]Organismal and Evolutionary Biology, University of Helsinki, P.O. Box 4, 00014 Helsinki, Finland

[3] Institute of Biotechnology, HiLIFE Helsinki Institute of Life Science, University of Helsinki, Helsinki 00014, Finland

[4] Department of Biological and Environmental Science, University of Jyväskylä, P.O. Box 35, FI-40014, University of Jyväskylä, Finland

[5] Department of Geosciences and Geography, University of Helsinki, PO BOX 55 00014 University of Helsinki, Finland

*Corresponding author: Natalie E. van Dis, ✉ natalie.vandis@helsinki.fi

ORCID ID: 0000-0002-9934-6751

Keywords: climate change, extreme climatic event, habitat heterogeneity, microclimate variability, population persistence, metapopulation dynamics

Abstract

As extreme climatic events are becoming more frequent and intense, we need to understand what mechanisms could buffer populations from climate change impacts to ensure their persistence. Fragmented populations may be especially vulnerable to climate change, as exemplified by species with metapopulation dynamics, whose persistence is determined by a precarious balance between frequent local extinctions and recolonizations of interconnected habitat patches. We investigated whether variation in vegetation productivity between and within habitat patches can buffer metapopulation dynamics in years of drought. Using 24 years of long-term monitoring data from the Glanville fritillary butterfly (*Melitaea cinxia*) for over 4000 habitat patches, we modelled temporal trends in butterfly habitat patch occupancy and abundance as a function of vegetation productivity and its heterogeneity during the growing season, using yearly Normalized Difference Vegetation Indices (NDVI) estimated from satellite data. We then tested whether these vegetation heterogeneity effects differed between years depending on the magnitude of drought, measured as the cumulative climatic water balance during the growing season. Across years, butterfly occupancy was consistently highest in patches with low to intermediate vegetation productivity. However, once patches were occupied, the effects of vegetation heterogeneity on butterfly abundances differed between years, showing opposite trends in dry vs wet years. In drier years, butterflies tended to be more abundant in patches of higher mean productivity, while in wet years, abundances tended to increase with higher levels of within-patch vegetation heterogeneity. These results indicate that there can be a mismatch between patch occupancy and abundance dynamics, with patch (re)colonization success not

responding to variation in the conditions that promote population growth during more extreme years. Nevertheless, our results suggest that differences in vegetation productivity within and between habitat patches can create enough variation in local population dynamics to support the metapopulation during extreme years. The type of vegetation heterogeneity needed for this support, however, varies with the type of climatic perturbation.

1. Introduction

Extreme climatic events such as extreme precipitation and droughts are rapidly increasing in frequency and intensity (IPCC, 2022). Such events can have severe consequences for population persistence, including widespread reproductive failure [e.g. (Schmidt et al., 2019)] and extreme mortality [e.g. (Garrabou et al., 2009)], that can result in population declines (Oliver et al., 2015; Piha et al., 2007). As biodiversity declines are starting to accelerate, we urgently need to implement conservation practices that buffer populations against climate change (Milles et al., 2023; Morelli et al., 2016). However, doing so requires a detailed understanding of the factors that can mitigate the severity of extreme event impacts on population persistence (Bailey & van de Pol, 2016; Van de Pol et al., 2017).

Fragmented populations may be especially vulnerable to extreme events, as climate change can exacerbate their risk of extinction (Opdam & Wascher, 2004; Travis, 2003). For example, during an extreme drought in Britain, drought-sensitive butterfly populations experienced more severe declines when residing in smaller habitat patches and slower population recovery when these habitat patches were more fragmented (Oliver et al., 2015). Such interactions between climate change and habitat configuration

67 can play a particularly important role for species with metapopulation dynamics, as

68 these populations are characterized by a balance between frequent local extinctions and

69 recolonizations (Hanski, 1999). Large environmental perturbations driven by climate

70 change may disrupt this precarious balance and can even cause metapopulation

71 extinction, as in the case of the Edith's checkerspot butterfly (*Euphydryas editha*) in

72 central California (Singer & Parmesan, 2010). Interestingly, other species with

73 metapopulation dynamics, including crickets, frogs, caddisflies and butterflies, have

74 experienced similar major declines in response to extreme climatic events but have so

75 far managed to persist [e.g. (Kindvall, 1996; Piha et al., 2007; Shama et al., 2011; van

76 Bergen et al., 2020)].

77 A metapopulation of the Glanville fritillary butterfly (*Melitaea cinxia*) in the Finnish

78 archipelago Åland has been extensively monitored since 1993, with its long-term data

79 spanning multiple climatic perturbations including an extreme summer drought (Fig.1),

80 making it an excellent system to investigate what buffering mechanisms could allow

81 metapopulations to persist. Modelling of the metapopulation consistently identifies

82 habitat area and connectivity as key factors explaining the observed population

83 dynamics, in combination with factors describing habitat quality [i.e. the abundance of

84 host plants and patch grazing intensity, (Hanski et al., 2017; Schulz et al., 2020)].

85 However, an increasing frequency of summer droughts is altering these dynamics, with

86 year-to-year population size fluctuations rising in amplitude and spatial synchrony

87 between local population dynamics increasing across the Åland islands, making the

88 metapopulation as a whole more vulnerable to extinction (Kahilainen et al., 2018; Tack et

89 al., 2015). Previous work indicated that population declines are likely mediated by larval

90 nutritional stress due to host plant quality changes in response to extreme drought

91   (Kahilainen et al., 2022; Salgado et al., 2020). We hypothesize that microhabitat variation

92   within and between patches is important for metapopulation persistence during summer

93   droughts, specifically variation in vegetation cover and productivity. Such habitat

94   heterogeneity can buffer populations against climate change through the availability of

95   microhabitats that remain suitable for survival and reproduction even under extreme

96   conditions, decreasing the risk of extinction (Milles et al., 2023; Suggitt et al., 2018). In *M.*

97   *cinxia*, a previous study found that patches with variation in the amount of shade were

98   more likely to have positive population growth rates in a year with a very dry and warm

99   spring, while this effect was absent in a year with a cooler spring (Rytteri et al., 2021).

100   However, the role of vegetation heterogeneity as a mechanism for buffering local

101   populations from extreme weather conditions has not yet been systematically assessed.
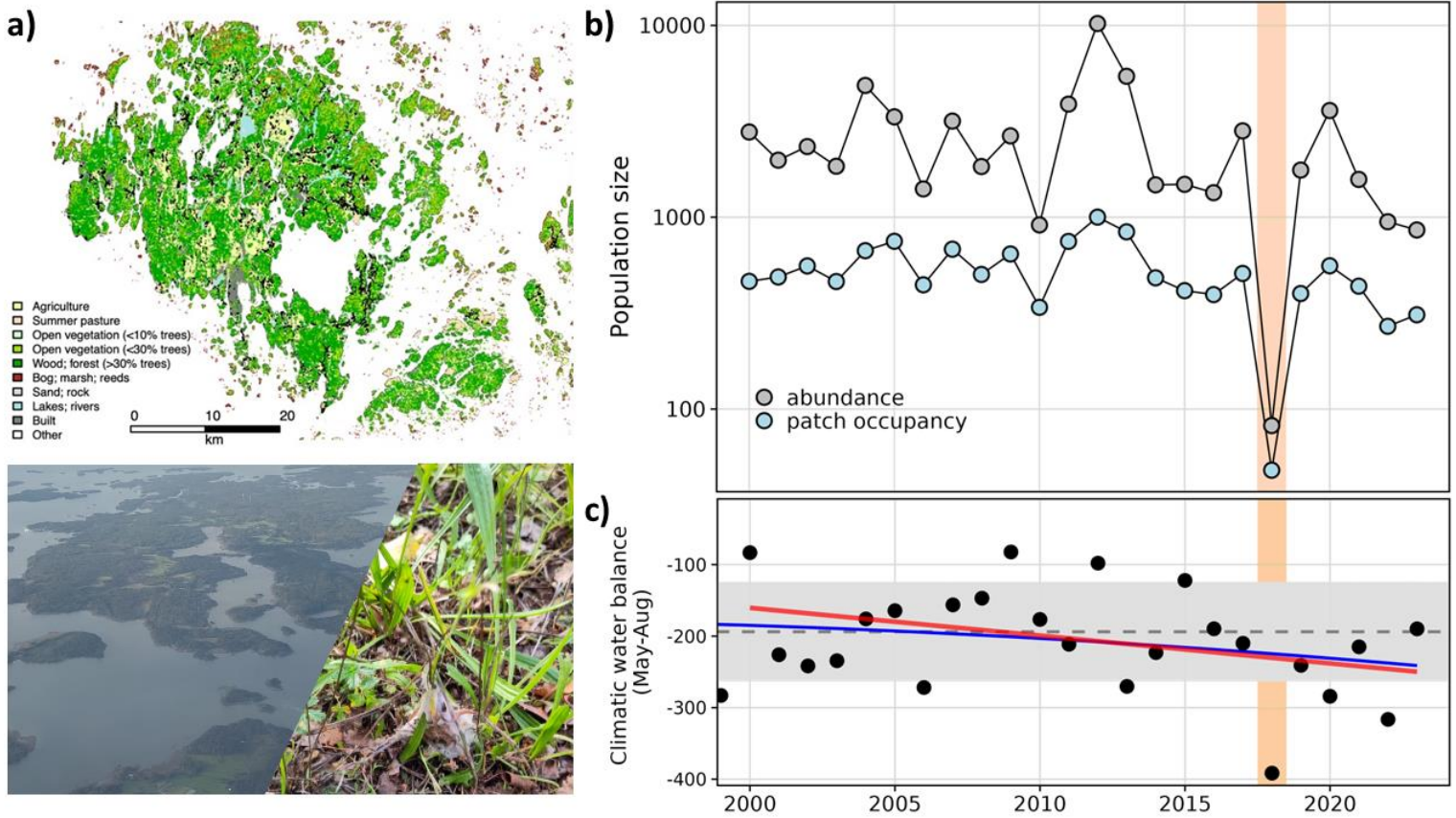
Figure 1. Temporal trends of Glanville fritillary butterfly (*Melitaea cinxia*) metapopulation dynamics in the Åland islands, Finland. Panel a) shows a map of the Åland islands colored by habitat / land use type with black points indicating the butterfly's potential habitat patches (N = 4395 meadows with one or both of the butterfly's host plants present), and below the map an aerial photo of the area and a photo of a *M. cinxia* larval nest (credits: NEvD). Panel b) depicts *M. cinxia* metapopulation dynamics 2000-2023 across these habitat patches, measured in autumn each year as patch occupancy (number of patches with at least one larval nest) and abundance (number of larval nests). Panel c) shows the drought magnitude per year for the same time period (black points) measured as cumulative climatic water balance during the butterfly's growing season (May-Aug, see Methods). The grey dashed line and shaded area give the long-term average ± 1 standard deviation and the blue line gives the long-term trend in drought magnitude (1959-2023), with 2018 being the driest year on record (see Fig.S1; extreme event highlighted in orange in panels b and c). For the period analyzed (2000-2023), the last eight years did not see any wetter than average years, with the red line giving the observed short-term trend of increasing drought during the growing season (estimate = -3.88, SE = 2.06, P = 0.07, Table S1).

Here, we investigate whether vegetation heterogeneity influences metapopulation persistence and growth in the Glanville fritillary butterfly (*Melitaea cinxia*), and how this

122   effect is modulated by drought magnitude. Using 24 years of long-term monitoring data

123   from a metapopulation in the Åland island archipelago in Finland (Fig.1), we modelled

124   temporal trends in butterfly habitat patch occupancy and abundance as a function of

125   vegetation productivity and its heterogeneity during the growing season, using yearly

126   Normalized Difference Vegetation Indices (NDVI) estimated from satellite data. We then

127   tested whether these vegetation heterogeneity effects differed between years depending

128   on the magnitude of drought, measured as the cumulative climatic water balance during

129   the growing season. While we expected that patches with higher vegetation productivity

130   would on average have lower butterfly occupancy and abundances across years, as *M.*

131   *cinxia* butterflies are considered to prefer more open meadows than overgrown ones in

132   the Åland islands (Ojanen et al., 2013), we expected that this effect might differ between

133   years, with higher vegetation productivity and within-patch heterogeneity (i.e., more

134   variation in NDVI between and within patches) promoting population survival especially

135   during dry years. Gaining insight into such drivers of population persistence is crucial for

136   understanding what determines population responses to ongoing climate change.

2. Methods

2.1 Long-term survey and climate data

139   Metapopulation dynamics of the Glanville fritillary butterfly (*Melitaea cinxia*) have been

140   monitored yearly since 1993 in the Åland islands, South-Western Finland (Hanski, 2011;

141   Ojanen et al., 2013). In this archipelago, the butterfly inhabits a network of over 4,000

142   potential habitat patches, typically dry meadows or pastures containing either one or

143   both of its host plants (ribwort plantain *Plantago lanceolata* and spiked speedwell

144   *Veronica spicata*, Fig.1). The butterflies are univoltine, with adults emerging in May and

145   females laying clutches of 150–200 eggs in June (Saastamoinen, 2007). The larvae hatch

146   in July to feed and develop up until the fourth instar, after which they overwinter in silken

147   'winter nests' as gregarious groups of mostly full-sib family groups (Fountain et al., 2018).

148   Every year, in late August to early September, each patch in the network is surveyed to

149   record butterfly occupancy and abundances (measured as the number of diapausing

150   larval groups, see Fig.1). The probability of missing an existing population (false negatives

151   for patch occupancy) is estimated to be around 10%, and these populations are mostly

152   very small [i.e. consisting of just one larval group; (Ojanen et al., 2013)]. For occupied

153   patches, around 50%–60% of all larval groups are detected (Hanski et al., 2017; Ojanen

154   et al., 2013). Our study focused on data collected in 2000-2023, as, from 2000 onwards,

155   the number of habitat patches surveyed yearly has remained stable and a standard set

156   of habitat variables has been recorded for each patch (Ojanen et al., 2013; Schulz et al.,

157   2020). These habitat variables include host plant abundances and grazing pressure,

158   which we combined with measures of patch area and connectivity in our analyses below.

159   For more details on the study system, see (Ojanen et al., 2013).

160   As an index of drought magnitude, we downloaded daily weather data (precipitation,

161   minimum and maximum temperature) for each survey year from the Finnish

162   Meteorological Institute (FMI) server (https://www.ilmatieteenlaitos.fi/havaintojen-

163   lataus) selecting the Jomala climate station in the Åland islands (60.12° N, 19.99° E, 11

164   m asl). We then calculated the potential evapotranspiration values per month based on

165   the monthly averages of observed minimum and maximum temperatures using the

166   Hargreaves method (Hargreaves, 1994) and computed the climatic water balance in mm

167   per month as mean precipitation minus mean potential evapotranspiration using R

168   v.4.4.2. (R Core Team, 2024) with package SPEI v.1.8.1. (Beguería et al., 2017) [for more

169   details, see (van Bergen et al., 2020)]. For each year, we took the sum of the monthly

170   climatic water balances May-August to obtain the climatic water balance accumulated

171   during the *M. cinxia* growing season.

2.2 Normalized Difference Vegetation Indices (NDVI)

173   We estimated the vegetation productivity of *M. cinxia* habitat patches using two types of

174   satellite data: Copernicus Sentinel-2 satellite data (2A and 2B satellites) by courtesy of

175   the European Space Agency (ESA) & Copernicus Program and satellite data from the

176   Landsat program (Landsat-5, 7, 8 and 9 satellites) by courtesy of the National Aeronautics

177   and Space Administration (NASA) and the United States Geological Survey (USGS). Both

178   surface reflectance datasets were accessed from the Google Earth Engine using R with

179   package rgee v.1.1.7 (Aybar et al., 2020). Sentinel data provided a finer resolution of 10m

180   and more frequent images, but were only available from 2016 onwards, so we used

181   Landsat data with a courser resolution of 30m for the full time series (2000-2023) and

182   Sentinel data for the years 2016-2023 to assess the impact of spatial resolution on the

183   results. From the satellite imagery, vegetation productivity during the growing season was

184   estimated for each patch and year by calculating the Normalized Difference Vegetation

185   Index (NDVI), a common proxy for vegetation greenness (Pettorelli et al., 2005). In short,

186   for each year, we downloaded available satellite scenes that were at least partly cloud-

187   free (maximum of 80% cloud cover) for the growing season months May-August [Sentinel:

188   N=467 scenes from 2016-2023; Landsat: N=343 scenes from 2000-2023]. We masked

189   pixels of poor quality by using the quality assessment (QA) layers available with the

190   satellite data and verified spatial accuracy for each scene visually. Additionally, we

191   created a unified water mask for the Landsat imagery by selecting 15 cloud-free images

192 and setting each pixel as water if for at least half of the selected images the focal pixel

193 was characterized as water in the corresponding QA-layer. Next, we calculated NDVI for

194 each pixel in the satellite images using the red and near-infrared satellite spectral bands

195 (i.e. estimating how green the vegetation is). The resulting NDVI rasters were visually

196 checked to exclude clearly erroneous images (e.g., due to failed cloud masks, N=5

197 Landsat scenes were excluded). Finally, we corrected for the effect of different satellite

198 sensors, as the different Landsat satellites have slightly varying spectral specifications

199 and NDVI is thus expected to show small systematic differences across the sensors

200 (Teillet et al., 2006). To do so, we identified scene pairs taken a maximum of five days

201 apart (i.e., image pairs of Landsat-5 ~ Landsat-7, Landsat-8 ~ Landsat-7, or Landsat-9 ~

202 Landsat-7). For each pair, we randomly sampled 50,000 overlapping clear pixels and

203 extracted the corresponding NDVI values. We then corrected the NDVI values across

204 sensors to match the Landsat-7 imagery scale, which temporally overlaps with the other

205 Landsat satellites, using linear models with the Landsat-7 values as the dependent

206 variable and the corresponding paired Landsat-5, 8 or 9 values as the independent

207 variable; extracting the predicted NDVI values from these models for further processing.

208 To account for potential temporal bias from interannual variation in the availability of

209 cloud-free imagery, both Landsat and Sentinel NDVI data were seasonally (i.e.,

210 phenologically) corrected using one GAM model per pixel (assuming a beta distribution

211 with a logit link function). These models included the raw NDVI values from each year as

212 the response variable, day of the year (continuous) as a fixed effect, a random intercept

213 for year (categorical), and a random slope for the interaction between day of the year and

214 year. We thus obtained seasonal NDVI curves for each year with a year-specific

215 correction for day of the year and extracted the predicted NDVI values for each day (May-

216   August) and year. Subsequently, vegetation productivity was calculated from the

217   seasonally corrected NDVI values, first for each pixel as the median NDVI pixel value per

218   month and year (Sentinel data, N=5.9±2.8 [average ± standard deviation] scenes per pixel

219   per month; Landsat data, N=3.5±2.0 scenes per pixel per month). Secondly, we

220   calculated for each patch the mean NDVI and its standard deviation per month and year,

221   using all pixels falling within that patch, to capture mean vegetation productivity and its

222   spatial within-patch heterogeneity, respectively. Finally, these monthly patch measures

223   were combined into one value per growing season (May-Aug) by taking the mean of the

224   monthly means and the root mean square of the monthly standard deviations, to use in

225   our analyses (see below). This three-step approach was used to ensure that each pixel

226   and each month contributed equally to the annual NDVI measures, to further reduce

227   potential bias arising from variation in the number of available satellite scenes. As the

228   monthly NDVI means and standard deviations could not be calculated for very small

229   patches that consisted of only one pixel in the Landsat data, and we know from previous

230   work that these patches have very little impact on the metapopulation dynamics of *M.*

231   *cinxia* (Hanski et al., 2017), these patches were excluded from the final analysis (on

232   average 5% of patches excluded per year).

2.3 Statistical analysis

234   To test whether vegetation heterogeneity influences metapopulation persistence and

235   growth in *M. cinxia* butterflies, we used generalized linear mixed models (GLMMs) in R

236   v.4.5.1 (R Core Team, 2025) using Bayesian latent gaussian models with integrated

237   nested Laplace approximation implemented in package INLA v.25.06.07 that enables

238   accounting for spatial autocorrelation (Rue et al., 2009). For each satellite data type, we

239   used two GLMMs to model *M. cinxia* metapopulation dynamics from 2000-2023 for

240   response variables: (1) annual patch occupancy [Bernoulli distribution] and (2) annual

241   larval nest abundance within occupied patches [negative binomial distribution]. For each

242   model, we included five fixed effects that previous work identified as major contributors

243   to *M. cinxia* metapopulation dynamics (Schulz et al., 2020), namely: patch habitat area,

244   population connectivity, host plant abundance per year, and patch population size in the

245   previous year (all log-transformed) and grazing intensity. To test for the effect of between-

246   patch variation in vegetation productivity, we included the annual mean Normalized

247   Difference Vegetation Index per patch as a fixed effect (mean NDVI, see above) as well as

248   mean NDVI squared to allow for nonlinear responses. To test for the effect of within-patch

249   vegetation heterogeneity, we included the annual NDVI standard deviation per patch as

250   a fixed effect. As host plants are a part of the vegetation and host plant availability in a

251   patch greatly influences the likelihood of butterfly occupancy (Schulz et al., 2020), we

252   also tested whether the effect of NDVI was mediated by host plant abundance by fitting

253   three interaction effects, one between each NDVI fixed effect and host plant abundance.

254   Before inclusion in the model, all fixed effects were standardized to a mean of zero and a

255   standard deviation of one.

256   Following previous work (Schulz et al., 2020), each model included year and patchID as

257   random effects, as well as a stochastic partial differentiation equation random effect

258   [SPDE, (Lindgren et al., 2011)] to account for spatial autocorrelation between patches.

259   We also fitted random year slopes for the three NDVI-based fixed effects and their

260   interactions with host plant abundance to obtain yearly NDVI effect sizes. We then used

261   linear models to test whether the magnitude of these yearly NDVI effect sizes depended

262   on the magnitude of drought. Here, we ran one model for each NDVI measure (i.e. mean
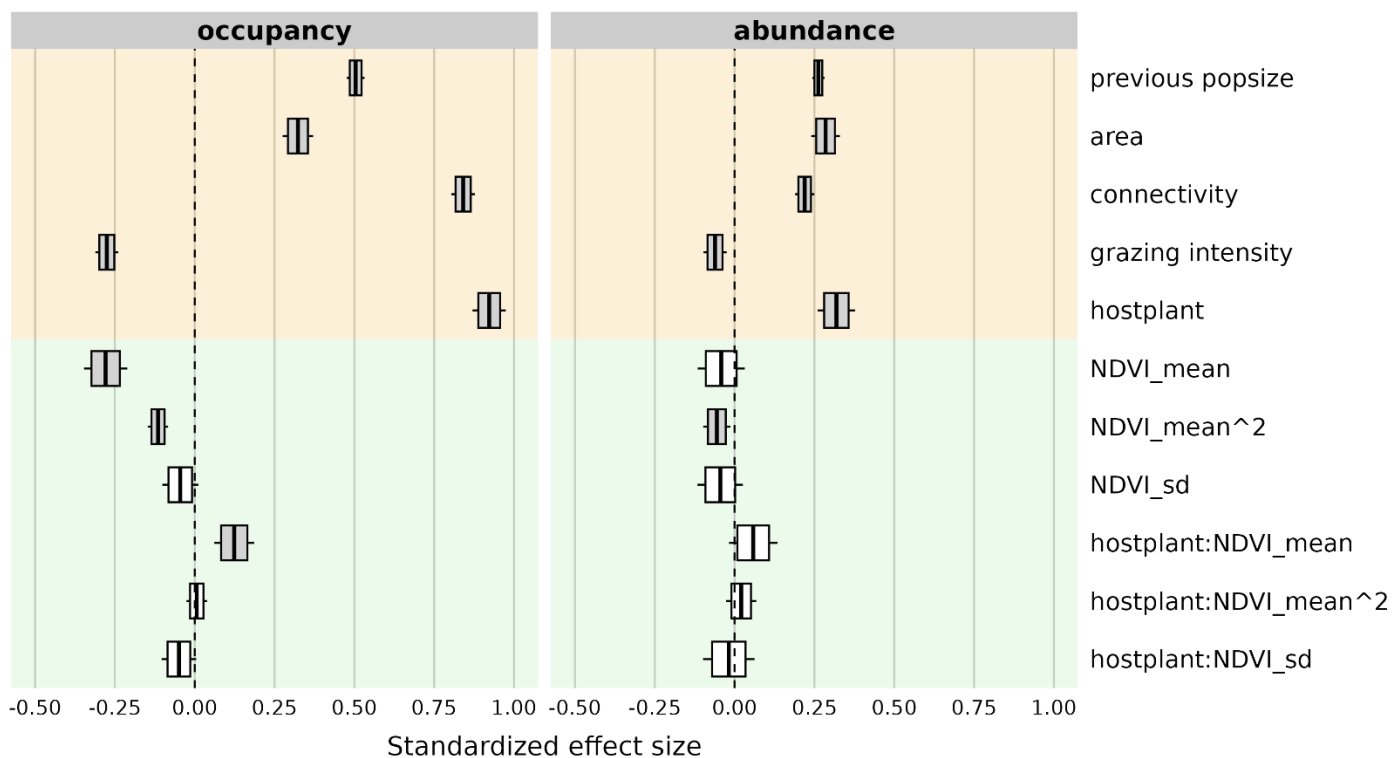
263   vegetation productivity, mean vegetation productivity squared, and vegetation

264   heterogeneity; and their interactions with host plant abundance), using the predicted

265   yearly slopes from the occupancy and abundance GLMMs as the response variable and

266   the cumulative climatic water balance and climatic water balance squared as fixed

267   effects. We ran both a linear model with only the point estimates (i.e. the mean of the

268   posterior mean distribution of each effect size estimate) and a linear model accounting

269   for the uncertainty around these estimates, by including the standard error of the

270   posterior mean distribution of each effect size estimate in the response variable using

271   package brms v.2.22.0 (Bürkner, 2017; Carpenter et al., 2017).

3. Results

### 3.1 Vegetation productivity and its heterogeneity affect butterfly population dynamics

275   Across years, butterfly patch occupancy and abundances were significantly impacted by

276   patch area, connectivity and quality (i.e. host plant abundance, and grazing intensity),

277   with both the direction and magnitude of effects consistent with previous work on this

278   system (Schulz et al., 2020): patches occupied in the previous year, as well as larger and

279   more connected patches with higher host plant abundances, had higher chances of

280   butterfly occupancy and higher abundances, while both occupancy and abundance

281   declined when patches were more intensely grazed (P<0.05, i.e. 95% Credible Intervals

282   [CI] do not overlap with zero, Fig.2, Table S2). Moreover, across years, patch occupancy,

283   but not butterfly abundance, was significantly impacted by between-patch variation in

284   vegetation productivity, in a nonlinear way and depending on host plant abundances

285   (P<0.05, Table S2). The effect sizes on patch occupancy of mean NDVI (i.e. Normalized

286   Difference Vegetation Index, see Methods) and mean NDVI squared during the butterfly's

287   growing season, as estimated from the Landsat satellite data, were both negative, while

288   the interaction between host plant abundance and mean NDVI was positive (Fig.2). These

289   effects were similar in direction and magnitude for the models in which NDVI variables

290   were based on higher resolution Sentinel satellite data, although these covered only a

291   subset of years (Fig. S2, Table S3).

292   **Figure 2. Standardized effect sizes of vegetation productivity and heterogeneity on**
293   **butterfly patch occupancy and abundance dynamics (2000-2023).** Both the
294   occupancy and abundance models contained five fixed effects previously found to
295   influence *M. cinxia* metapopulation dynamics (i.e. covariates highlighted in orange:
296   population size in the previous year, patch area, connectivity, grazing intensity, and host
297   plant abundances) as well as fixed effects capturing between-patch variation in
298   vegetation productivity and within-patch vegetation heterogeneity (highlighted in green),
299   as estimated from Landsat satellite data by the mean Normalized Difference Vegetation
300   Index (NDVI), mean NDVI squared and NDVI standard deviation (sd) per patch (see
301   Methods). For each fixed effect the posterior means are shown with boxes depicting the
302   80% Credible Intervals [CI] and whiskers the 95% CIs, colored grey when the 95% CIs did
303   not overlap with zero (i.e. P<0.05, Table S2).
304

305   The effect of mean NDVI on patch occupancy followed an inverse U-shape relationship

306   (Fig.3), where the odds of patch occupancy were maximized at low to intermediate levels

307   of vegetation productivity but decreased for lower or higher mean NDVI. The significant

308   interaction between host plant abundance and mean NDVI furthermore meant that the

309   odds of patch occupancy were maximized at a higher NDVI mean when patches had

310   higher host plant abundances (Fig.3). For abundance, the effect of mean NDVI did not

311   differ from zero but we did find a significant negative effect of NDVI squared albeit with a

312   smaller effect size than the occupancy model ($P<0.05$, Fig.2), meaning that butterfly

313   abundances tended to be slightly higher for patches with intermediate levels of

314   vegetation productivity across years. The effect of within-patch vegetation heterogeneity

315   on patch occupancy and abundances, measured as the NDVI standard deviation (sd) of

316   each patch (see Methods), was similarly negative but did not differ from zero (Fig.2).
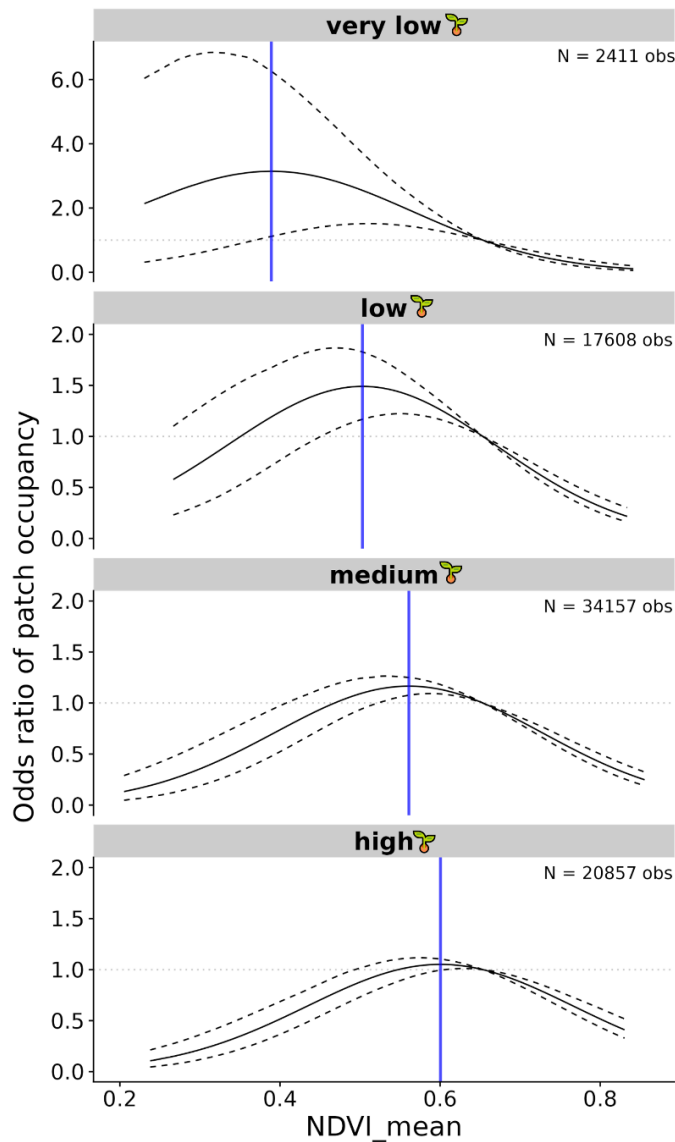
Figure 3. Effect of mean Normalized Difference Vegetation Index (NDVI) during the growing season (May-Aug) on butterfly patch occupancy odds ratios. The posterior means of the combined effects of mean NDVI, mean NDVI squared, and the interaction between mean NDVI and host plant abundance (black lines) – found to significantly impact the chances of patch occupancy (see Fig.2) – are depicted with their 95% Credible Intervals (CI, black dashed lines), while keeping all other fixed effects in the model at reference level (i.e. their average values across years). An odds ratio of one (grey dotted line) refers to the odds of patch occupancy at reference level. The effect of mean NDVI is split into four groups of host plant abundance levels (measured in the field on an ordinal scale 0-3: very low, low, medium, and high) to show the interaction between mean NDVI and host plant abundance: the mean NDVI at which the odds of patch occupancy was maximized (blue lines) increased for patches with higher host plant abundances. The numbers of observations (number of year-patch combinations) underlying the patterns for each panel are reported in the top right corners. Note the different y-scale for the very low host plant abundance panel.

3.2 Vegetation heterogeneity effect size modulation by drought

Using the yearly fitted random slopes of the vegetation productivity fixed effects (i.e. Normalized Difference Vegetation Index [NDVI] measures) and their interactions with host plant abundance from the Landsat occupancy and abundance models (Fig.2), we tested whether the magnitude of the NDVI effect sizes on butterfly population dynamics differed between years depending on the magnitude of drought during the growing season (May-Aug). While between-patch variation in vegetation productivity (mean NDVI) affected patch occupancy dynamics across years (Fig.2), the effect sizes of mean NDVI and mean NDVI squared on patch occupancy did not differ between years according to drought magnitude. Similarly, neither the effect size of within-patch vegetation heterogeneity (NDVI standard deviation [sd]) nor those of the interactions of NDVI with host plant abundance were affected by drought magnitude ($P>0.10$, Fig.S4, Table S5). In contrast, we did find NDVI effect size modulation by drought of patch abundance dynamics. While across years, butterfly patch abundances were not significantly impacted by mean NDVI (Fig.2), the yearly effect sizes showed a trend whereby drier years had more positive effect sizes and wetter years had more negative effect sizes. The same linear trend was apparent for mean NDVI in interaction with host plant abundance ($P<0.10$ in the simple linear models, Fig.4, Table S6). Thus, while higher mean vegetation productivity led to lower butterfly patch abundances in wetter years, in drier years butterfly abundances were higher for the same mean vegetation productivity. However, these modulation effects were not robust to uncertainty in the posterior mean effect sizes, as the effect of drought magnitude on the mean NDVI effect sizes no longer differed from zero after accounting for the standard deviations around the posterior means ($P>0.10$ in the more complex linear models, Fig.4, Table S6).

17
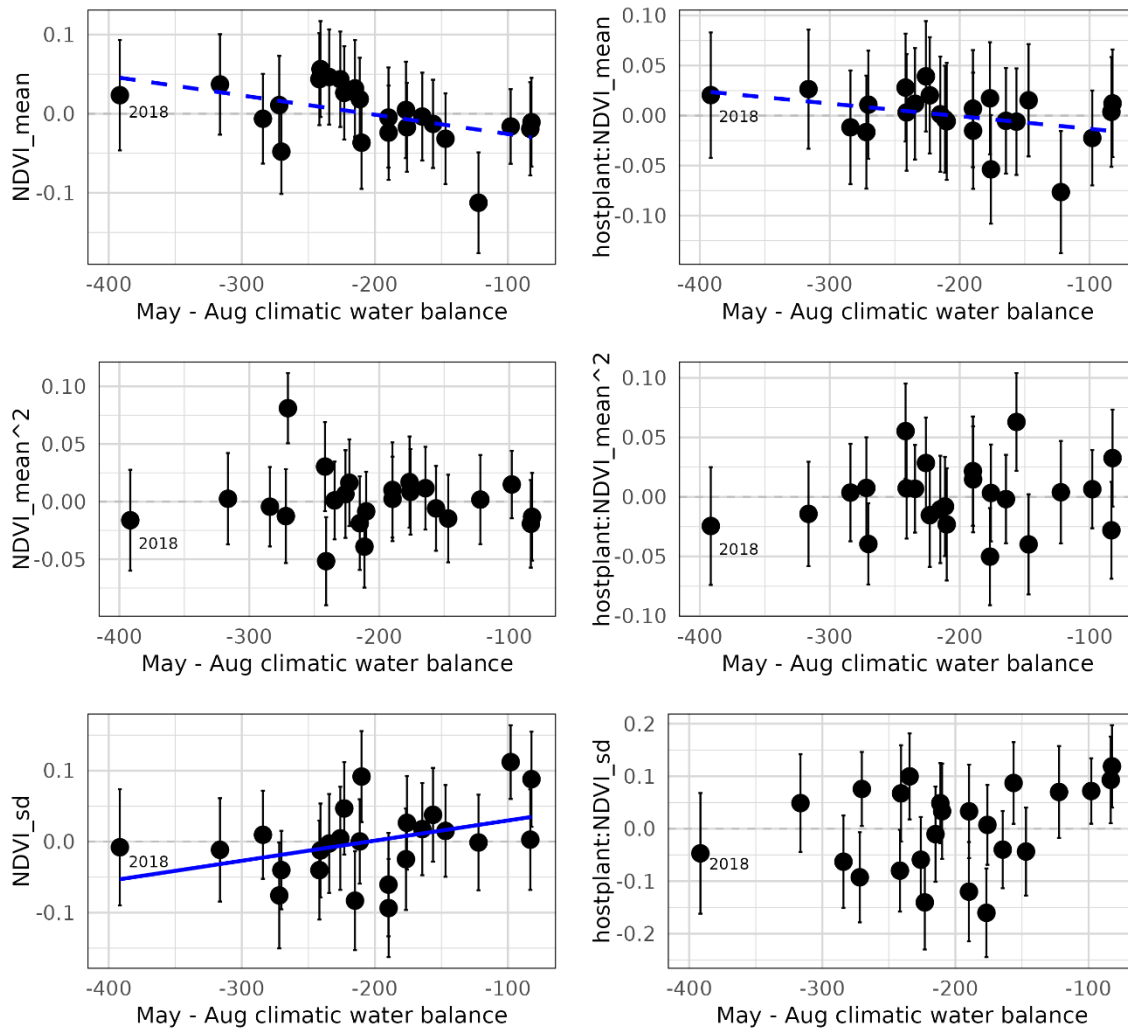
Figure 4. Vegetation productivity and heterogeneity effect sizes on butterfly abundance modulated by drought magnitude. Each panel shows the relationship between drought magnitude on the x-axis (measured as the cumulative climatic water balance in mm during the butterfly growing season May-Aug) and on the y-axis the yearly slope effect sizes of each Normalized Difference Vegetation Index (NDVI) fixed effect and their interactions with host plant abundance on patch abundance (see Fig.2 for the fixed effect model coefficients). Points are the posterior mean year slope effect sizes ± posterior standard deviation. Blue lines indicate significant trends of drought magnitude and/or drought magnitude squared on NDVI effect sizes (P<0.10), with dashed lines indicating trends that were only found in simple linear models and solid lines indicating trends that remained when also modelling the uncertainty around the posterior effect size means (see Methods, Table S6).

In addition to drought modulation of mean NDVI effect sizes, we found an effect of

drought magnitude on the yearly effect sizes of within-patch vegetation heterogeneity

(NDVI sd) on patch abundances, but in the opposite direction. In dry years, NDVI sd effect

375   sizes on patch abundances were more negative, thus patches with more within-patch

376   variation in vegetation productivity tended to have lower butterfly abundances in dry

377   years, while in wetter years patches tended to have higher abundances for the same

378   levels of within-patch vegetation heterogeneity (P<0.10, Fig.4, Table S6). This drought

379   modulation effect was robust both to estimate uncertainty and to the effect of the 2018

380   extreme event, as the trend remained when accounting for the standard deviations

381   around the posterior mean effect sizes and when excluding 2018 from the analysis

382   (P<0.10, Table S6).

4. Discussion

384   As the frequency and intensity of extreme climatic events are increasing, a pressing

385   question is what mechanisms could buffer populations from climate change impacts to

386   ensure their persistence (Milles et al., 2023; Morelli et al., 2016). Such buffering might be

387   especially important for metapopulations that persist in a precarious balance between

388   frequent local extinctions and recolonizations of interconnected habitat patches, as

389   climate change could trigger synchronized local population collapses that drive the

390   metapopulation to extinction (Hanski, 1999). We investigated whether variation in

391   vegetation productivity between and within habitat patches can buffer metapopulation

392   dynamics, and whether these effects differed between years depending on the

393   magnitude of drought. Using 24 years of data from the Glanville fritillary butterfly

394   (*Melitaea cinxia*) as our model system, we found that vegetation productivity affected

395   occupancy dynamics in a similar way across years, while once patches were occupied,

396   the effects of vegetation productivity and its within-patch heterogeneity on butterfly

397   abundances differed between years depending on drought magnitude.

398   In line with our expectations, across years, patches with higher vegetation productivity

399   consistently had lower chances of butterfly occupancy, with this effect being modulated

400   by the number of host plants available in the patch (Fig. 2 and 3). Between-patch variation

401   in vegetation productivity thus seems to decrease habitat suitability for *M. cinxia*. Indeed,

402   in the Åland islands, *M. cinxia* butterflies tend to occur more in open meadows than

403   overgrown ones (Ojanen et al., 2013) and females preferentially oviposit in microhabitats

404   with higher host plant abundances (Salgado et al., 2020). More homogeneous habitat is

405   generally considered to be beneficial for species that are sensitive to habitat quality, such

406   as specialist species with strict habitat requirements and species with low dispersal

407   capability (Donaldson et al., 2017; Ye et al., 2013) and diversification of such habitats can

408   lead to local extinctions of specialist species (Habel et al., 2019). Interestingly, however,

409   while vegetation heterogeneity effects on occupancy dynamics did not differ between

410   years depending on drought magnitude, we found the opposite to be true for patch

411   abundances (Fig. 4). Thus, in both dry and wet years, oviposition preferences and/or

412   establishment success of the butterfly were highest for patches with low to intermediate

413   vegetation productivity levels, but once occupied, the effects of between and within

414   patch vegetation heterogeneity on butterfly abundances differed between years

415   depending on drought magnitude.

416   Our *a priori* expectation was that vegetation heterogeneity would promote population

417   survival in drier years, but the effects of between- and within-patch variation in vegetation

418   productivity on butterfly abundances in fact showed opposite trends (Fig. 4). In line with

419   our expectations, vegetation productivity had a more positive effect on butterfly

420   abundances in drier years. The same trend was also found for the interaction between

421   vegetation productivity and host plant abundances, meaning that more productive

422   patches tended to have higher butterfly abundances than less productive patches in dry

423   years. While not robust to uncertainty in the annual estimates, this pattern suggests that

424   in drier years more productive patches were more likely to retain sufficient (high quality)

425   host plants and/or beneficial microhabitats to support larval development. Thus,

426   variation in vegetation productivity between patches could buffer the metapopulation by

427   ensuring butterfly survival in at least some patches in years of more extreme drought.

428   In contrast, within-patch vegetation heterogeneity had a more positive effect on butterfly

429   abundance not in drier but in wetter years, meaning that butterfly abundances tended to

430   be higher in more heterogeneous patches in wet years. This effect was robust to estimate

431   uncertainty and opposite to our *a priori* expectation that within-patch variation might

432   similarly promote butterfly survival in dry years by providing microhabitats that support

433   larval development. It may be that this effect instead captures the effect of within-patch

434   variation in vegetation height, for example mediated by the presence of more rocky terrain

435   or shade, which might be more important in wet years than dry years. Indeed, in wetter

436   years, we expect the vegetation to grow higher, leading to more overgrown habitat that is

437   considered to be poor habitat for species whose egg and larval development rely on

438   warm microclimates (WallisDeVries & van Swaay, 2006). Previous work found that *M.*

439   *cinxia* not only prefers more open microhabitats, but also drier microhabitats in the Åland

440   islands, preferentially laying eggs on host plants with signs of drought stress, which might

441   be attributed to the fact that the butterfly occurs at its most northern range edge in this

442   archipelago and thus might select warmer microhabitats for egg laying to facilitate larval

443   development (Salgado et al., 2020). These results thus suggest that variation in

444   vegetation productivity within patches may buffer the metapopulation on the opposite

445   end of weather extremes. In wet years, when high vegetation productivity causes patches

446   to become overgrown, more open microhabitats could help ensure butterfly survival.

447   Habitat heterogeneity has been previously associated with more stable population

448   dynamics, suggesting that heterogeneous landscapes can buffer populations against

449   climatic variation (Oliver et al., 2010). Our results provide insight into when, i.e., under

450   which conditions, habitat heterogeneity can buffer populations against such climatic

451   perturbations. Specifically, we found that the type and degree of heterogeneity that is

452   optimal may differ between average, wet and dry years. Importantly, our results

453   corroborate that in average years, homogeneous low-productive seminatural grasslands

454   are essential for the preservation of species relying on warm microclimates

455   (WallisDeVries & van Swaay, 2006; Warren et al., 2021). But our results also show that

456   more heterogenous habitats, which in average years are less suitable for population

457   persistence and survival, can become important during climatic perturbations and

458   extreme events. This is likely to apply not only to Lepidoptera species but also to other

459   drought-sensitive taxa, such as crickets, frogs, and caddisflies [e.g. (Kindvall, 1996; Piha

460   et al., 2007; Shama et al., 2011)]. Moreover, our results suggest a potential mismatch

461   between patch occupancy and patch abundance dynamics, with patch (re)colonization

462   success not responding to variation in the conditions that promote population growth

463   during more extreme years. Such a mismatch might be the result of oviposition behavior,

464   with females unable to predict or respond to variation in the habitat conditions that best

465   support larval growth and survival later in the season, as previous work found that female

466   habitat preference for oviposition did not differ between an average and an extremely dry

467   year, while the type of habitat that best supported larval survival differed between these

468   years (Salgado et al., 2020).

469 Our analyses test the hypothesis that the severity of climate change effects on

470 metapopulation dynamics are mediated through vegetation productivity, whereby

471 variation in vegetation productivity promotes microclimatic variation that can buffer

472 butterfly survival and development during periods of extreme weather, likely through their

473 effects on host plant quality and abundance (Kahilainen et al., 2022; Rytteri et al., 2021;

474 Salgado et al., 2020). While our results support a role of vegetation heterogeneity in

475 buffering populations from climate change, further work is needed to determine what

476 drives between- and within-patch vegetation heterogeneity [e.g., soil type, topographic

477 variation, or presence of trees, shrubs, and forest edges that provide shade (Ojanen et

478 al., 2013; Salgado et al., 2020)]. Other factors outside the scope of our study, such as

479 variation in topography or solar radiation, may also create microclimatic heterogeneity

480 independently of vegetation structure and cover (Suggitt et al., 2018).

5. Conclusion

482 A major concern for metapopulation persistence under climate change is increased

483 synchrony in local population declines, which reduces the number of local populations

484 that sustain the extinction-recolonization balance to prevent metapopulation extinction

485 (Hanski, 1999; Kahilainen et al., 2018). Our results indicate that while, on average,

486 vegetation heterogeneity is not necessarily beneficial for population persistence and

487 growth, variation in vegetation productivity both between and within habitat patches

488 could introduce sufficient variation in local population dynamics to buffer the

489 metapopulation during extreme years. The type of vegetation heterogeneity required for

490 buffering, however, seems to depend on the climatic perturbation. As extreme events are

491 expected to keep increasing in frequency and intensity with ongoing climate change

492 (IPCC, 2022), conservation practices should thus not only focus on maintaining and

493 increasing the availability of high-quality habitat but also on maintaining and promoting

494 a degree of habitat heterogeneity. Based on our results, we suggest that for drought-

495 sensitive species that depend on warm microclimates for development (WallisDeVries &

496 van Swaay, 2006; Warren et al., 2021), high quality habitat includes low-productivity, well-

497 connected meadows with high host plant abundances. In addition, our results indicate

498 that landscape elements that promote open habitat features, and thus within-patch

499 variation in vegetation height, may promote population survival especially in wet years.

500 In contrast, in dry years, the availability of drought-resilient habitat patches with higher

501 vegetation productivity, for example, mediated by soil type, topographic variation, or the

502 presence of shade, may be essential for population growth.

Declarations

511 The authors declare no competing or financial interests.

Data availability statement

All data and code used for analysis are available in the Zenodo repository

[https://doi.org/10.5281/zenodo.17790396] (van Dis et al., 2025).

Author contributions

N.E.v.D.: data analysis and visualization, writing – original draft; M.J.: conceptualization, data curation, data analysis, writing – review and editing; P.N.: methodology (satellite data processing and NDVI calculation), writing – review and editing; M.L.: methodology (climatic water balance calculation), writing – review and editing; J.S.: advice on data analysis, writing – review and editing; M.S.: conceptualization, funding acquisition, supervision, writing – review and editing.

References

Aybar, C., Wu, Q., Bautista, L., Yali, R., & Barja, A. (2020). rgee: An R package for interacting with Google Earth Engine. *Journal of Open Source Software*, *5*(51), 2272. https://doi.org/10.21105/joss.02272

Bailey, L. D., & van de Pol, M. (2016). Tackling extremes: Challenges for ecological and evolutionary research on extreme climatic events. *Journal of Animal Ecology*, *85*(1), 85–96. https://doi.org/10.1111/1365-2656.12451

Beguería, S., Vicente-Serrano, S. M., & Beguería, M. S. (2017). *Package 'spei'. Calculation of the Standardised Precipitation-Evapotranspiration Index*. CRAN [Package].

Bürkner, P.-C. (2017). brms: An R Package for Bayesian Multilevel Models Using Stan. *Journal of Statistical Software*, *80*(1), 1–28. https://doi.org/doi:10.18637/jss.v080.i01

Carpenter, B., Gelman, A., Hoffman, M. D., Lee, D., Goodrich, B., Betancourt, M., Brubaker, M. A., Guo, J., Li, P., & Riddell, A. (2017). Stan: A probabilistic programming language. *Journal of Statistical Software*, *76*(1). https://doi.org/10.18637/jss.v076.i01

Donaldson, L., Wilson, R. J., & Maclean, I. M. D. (2017). Old concepts, new challenges: adapting landscape-scale conservation to the twenty-first century. *Biodiversity and Conservation*, *26*(3), 527–552. https://doi.org/10.1007/s10531-016-1257-9

Fountain, T., Husby, A., Nonaka, E., DiLeo, M. F., Korhonen, J. H., Rastas, P., Schulz, T., Saastamoinen, M., & Hanski, I. (2018). Inferring dispersal across a fragmented landscape

541   using reconstructed families in the Glanville fritillary butterfly. *Evolutionary Applications*,
542   *11*(3), 287–297. https://doi.org/10.1111/eva.12552

543   Garrabou, J., Coma, R., Bensoussan, N., Bally, M., Chevaldonné, P., Cigliano, M., Diaz, D.,
544   Harmelin, J. G., Gambi, M. C., Kersting, D. K., Ledoux, J. B., Lejeusne, C., Linares, C.,
545   Marschal, C., Pérez, T., Ribes, M., Romano, J. C., Serrano, E., Teixido, N., … Cerrano, C.
546   (2009). Mass mortality in Northwestern Mediterranean rocky benthic communities: Effects
547   of the 2003 heat wave. *Global Change Biology*, *15*(5), 1090–1103.
548   https://doi.org/10.1111/j.1365-2486.2008.01823.x

549   Habel, J. C., Segerer, A. H., Ulrich, W., & Schmitt, T. (2019). Succession matters: Community
550   shifts in moths over three decades increases multifunctionality in intermediate
551   successional stages. *Scientific Reports*, *9*(1), 1–8. https://doi.org/10.1038/s41598-019-
552   41571-w

553   Hanski, I. (1999). *Metapopulation ecology*. Oxford University Press.

554   Hanski, I. (2011). Eco-evolutionary spatial dynamics in the Glanville fritillary butterfly.
555   *Proceedings of the National Academy of Sciences of the United States of America*, *108*(35),
556   14397–14404. https://doi.org/10.1073/pnas.1110020108

557   Hanski, I., Schulz, T., Wong, S. C., Ahola, V., Ruokolainen, A., & Ojanen, S. P. (2017). Ecological
558   and genetic basis of metapopulation persistence of the Glanville fritillary butterfly in
559   fragmented landscapes. *Nature Communications*, *8*.
560   https://doi.org/10.1038/ncomms14504

561   Hargreaves, G. H. (1994). Defining and using reference evapotranspiration. *Journal of Irrigation*
562   *and Drainage Engineering*, *129*, 1132–1139.

563   IPCC. (2022). *Climate Change 2022: Impacts, Adaptation and Vulnerability; Summary for*
564   *policymakers*. https://doi.org/10.4324/9781315071961-11

565   Kahilainen, A., Oostra, V., Somervuo, P., Minard, G., & Saastamoinen, M. (2022). Alternative
566   developmental and transcriptomic responses to host plant water limitation in a butterfly
567   metapopulation. *Molecular Ecology*, *31*(22), 5666–5683.
568   https://doi.org/10.1111/mec.16178

569   Kahilainen, A., van Nouhuys, S., Schulz, T., & Saastamoinen, M. (2018). Metapopulation
570   dynamics in a changing climate: Increasing spatial synchrony in weather conditions drives
571   metapopulation synchrony of a butterfly inhabiting a fragmented landscape. *Global*
572   *Change Biology*, *24*(9), 4316–4329. https://doi.org/10.1111/gcb.14280

573   Kindvall, O. (1996). Habitat Heterogeneity and Survival in a Bush Cricket Metapopulation.
574   *Ecology*, *77*(1), 207–214. https://doi.org/10.2307/2265670

575   Lindgren, F., Rue, H., & Lindström, J. (2011). An explicit link between gaussian fields and
576   gaussian markov random fields: The stochastic partial differential equation approach.
577   *Journal of the Royal Statistical Society. Series B: Statistical Methodology*, *73*(4), 423–498.
578   https://doi.org/10.1111/j.1467-9868.2011.00777.x

579   Milles, A., Banitz, T., Bielcik, M., Frank, K., Gallagher, C. A., Jeltsch, F., Jepsen, J. U., Oro, D.,
580   Radchuk, V., & Grimm, V. (2023). Local buffer mechanisms for population persistence.

581   *Trends in Ecology and Evolution*, *38*(11), 1051–1059.
582   https://doi.org/10.1016/j.tree.2023.06.006

583 Morelli, T. L., Daly, C., Dobrowski, S. Z., Dulen, D. M., Ebersole, J. L., Jackson, S. T., Lundquist, J.
584   D., Millar, C. I., Maher, S. P., Monahan, W. B., Nydick, K. R., Redmond, K. T., Sawyer, S. C.,
585   Stock, S., & Beissinger, S. R. (2016). Managing climate change refugia for climate
586   adaptation. *PLoS ONE*, *11*(8), 1–17. https://doi.org/10.1371/journal.pone.0159909

587 Ojanen, S. P., Nieminen, M., Meyke, E., Pöyry, J., & Hanski, I. (2013). Long-term metapopulation
588   study of the Glanville fritillary butterfly (Melitaea cinxia): Survey methods, data
589   management, and long-term population trends. *Ecology and Evolution*, *3*(11), 3713–3737.
590   https://doi.org/10.1002/ece3.733

591 Oliver, T. H., Marshall, H. H., Morecroft, M. D., Brereton, T., Prudhomme, C., & Huntingford, C.
592   (2015). Interacting effects of climate change and habitat fragmentation on drought-
593   sensitive butterflies. *Nature Climate Change*, *5*(10), 941–946.
594   https://doi.org/10.1038/nclimate2746

595 Oliver, T. H., Roy, D. B., Hill, J. K., Brereton, T., & Thomas, C. D. (2010). Heterogeneous
596   landscapes promote population stability. *Ecology Letters*, *13*(4), 473–484.
597   https://doi.org/10.1111/j.1461-0248.2010.01441.x

598 Opdam, P., & Wascher, D. (2004). Climate change meets habitat fragmentation: Linking
599   landscape and biogeographical scale levels in research and conservation. *Biological*
600   *Conservation*, *117*(3), 285–297. https://doi.org/10.1016/j.biocon.2003.12.008

601 Pettorelli, N., Vik, J. O., Mysterud, A., Gaillard, J.-M., Tucker, C. J., & Stenseth, N. C. (2005). Using
602   the satellite-derived NDVI to assess ecological responses to environmental change. *Trends*
603   *in Ecology & Evolution*, *20*(9), 503–510. https://doi.org/10.1016/j.tree.2005.05.011

604 Piha, H., Luoto, M., Piha, M., & Merilä, J. (2007). Anuran abundance and persistence in
605   agricultural landscapes during a climatic extreme. *Global Change Biology*, *13*(1), 300–311.
606   https://doi.org/10.1111/j.1365-2486.2006.01276.x

607 R Core Team. (2024). *R: A language and environment for statistical computing*. R Foundation for
608   Statistical Computing.

609 R Core Team. (2025). *R: A language and environment for statistical computing*. R Foundation for
610   Statistical Computing.

611 Rue, H., Martino, S., & Chopin, N. (2009). Approximate Bayesian Inference for Latent Gaussian
612   models by using Integrated Nested Laplace Approximations. *Journal of the Royal Statistical*
613   *Society Series B: Statistical Methodology*, *71*(2), 319–392. https://doi.org/10.1111/j.1467-
614   9868.2008.00700.x

615 Rytteri, S., Kuussaari, M., & Saastamoinen, M. (2021). Microclimatic variability buffers butterfly
616   populations against increased mortality caused by phenological asynchrony between
617   larvae and their host plants. *Oikos*, *130*(5), 753–765. https://doi.org/10.1111/oik.07653

618 Saastamoinen, M. (2007). Life-history, genotypic, and environmental correlates of clutch size in
619   the Glanville fritillary butterfly. *Ecological Entomology*, *32*(2), 235–242.
620   https://doi.org/10.1111/j.1365-2311.2007.00865.x

621   Salgado, A. L., DiLeo, M. F., & Saastamoinen, M. (2020). Narrow oviposition preference of an
622   insect herbivore risks survival under conditions of severe drought. *Functional Ecology*,
623   *34*(7), 1358–1369. https://doi.org/10.1111/1365-2435.13587

624   Schmidt, N. M., Reneerkens, J., Christensen, J. H., Olesen, M., & Roslin, T. (2019). An
625   ecosystem-wide reproductive failure with more snow in the Arctic. *PLoS Biology*, *17*(10), 1–
626   8. https://doi.org/10.1371/journal.pbio.3000392

627   Schulz, T., Vanhatalo, J., & Saastamoinen, M. (2020). Long-term demographic surveys reveal a
628   consistent relationship between average occupancy and abundance within local
629   populations of a butterfly metapopulation. *Ecography*, *43*(2), 306–317.
630   https://doi.org/10.1111/ecog.04799

631   Shama, L. N., Kubow, K. B., Jokela, J., & Robinson, C. T. (2011). Bottlenecks drive temporal and
632   spatial genetic changes in alpine caddisfly metapopulations. *BMC Evolutionary Biology*,
633   *11*, 278. https://doi.org/10.1186/1471-2148-11-278

634   Singer, M. C., & Parmesan, C. (2010). Phenological asynchrony between herbivorous insects
635   and their hosts: signal of climate change or pre-existing adaptive strategy? *Phil. Trans. R.*
636   *Soc. B*, *365*, 3161–3176. https://doi.org/10.1098/rstb.2010.0144

637   Suggitt, A. J., Wilson, R. J., Isaac, N. J. B., Beale, C. M., Auffret, A. G., August, T., Bennie, J. J.,
638   Crick, H. Q. P., Duffield, S., Fox, R., Hopkins, J. J., Macgregor, N. A., Morecroft, M. D.,
639   Walker, K. J., & Maclean, I. M. D. (2018). Extinction risk from climate change is reduced by
640   microclimatic buffering. *Nature Climate Change*, *8*(8), 713–717.
641   https://doi.org/10.1038/s41558-018-0231-9

642   Tack, A. J. M., Mononen, T., & Hanski, I. (2015). Increasing frequency of low summer
643   precipitation synchronizes dynamics and compromises metapopulation stability in the
644   Glanville fritillary butterfly. *Proceedings of the Royal Society B: Biological Sciences*,
645   *282*(1806). https://doi.org/10.1098/rspb.2015.0173

646   Teillet, P. M., Markham, B. L., & Irish, R. R. (2006). Landsat cross-calibration based on near
647   simultaneous imaging of common ground targets. *Remote Sensing of Environment*, *102*(3–
648   4), 264–270. https://doi.org/10.1016/j.rse.2006.02.005

649   Travis, J. M. J. (2003). Climate change and habitat destruction: A deadly anthropogenic cocktail.
650   *Proceedings of the Royal Society B: Biological Sciences*, *270*(1514), 467–473.
651   https://doi.org/10.1098/rspb.2002.2246

652   van Bergen, E., Dallas, T., DiLeo, M. F., Kahilainen, A., Mattila, A. L. K., Luoto, M., &
653   Saastamoinen, M. (2020). The effect of summer drought on the predictability of local
654   extinctions in a butterfly metapopulation. *Conservation Biology*, *34*(6), 1503–1511.
655   https://doi.org/10.1111/cobi.13515

656   Van de Pol, M., Jenouvrier, S., Cornelissen, J. H. C., & Visser, M. E. (2017). Behavioural,
657   ecological and evolutionary responses to extreme climatic events: Challenges and
658   directions. *Philosophical Transactions of the Royal Society B: Biological Sciences*,
659   *372*(1723). https://doi.org/10.1098/rstb.2016.0134

660   van Dis, N. E., Jones, M. M., Niittynen, P., Luoto, M., Siren, J., & Saastamoinen, M. (2025).
661   Butterfly abundances but not patch occupancy buffered by vegetation heterogeneity
662   during climatic extremes. *Zenodo*, *Dataset*. https://doi.org/10.5281/zenodo.17790396

663 WallisDeVries, M. F., & van Swaay, C. A. M. (2006). Global warming and excess nitrogen may
664   induce butterfly decline by microclimatic cooling. *Global Change Biology*, *12*(9), 1620–
665   1626. https://doi.org/10.1111/j.1365-2486.2006.01202.x

666 Warren, M. S., Maes, D., van Swaay, C. A. M., Goffart, P., van Dyck, H., Bourn, N. A. D., Wynhoff,
667   I., Hoare, D., & Ellis, S. (2021). The decline of butterflies in Europe: Problems, significance,
668   and possible solutions. *Proceedings of the National Academy of Sciences of the United*
669   *States of America*, *118*(2), 1–10. https://doi.org/10.1073/PNAS.2002551117

670 Ye, X., Skidmore, A. K., & Wang, T. (2013). Within-patch habitat quality determines the resilience
671   of specialist species in fragmented landscapes. *Landscape Ecology*, *28*(1), 135–147.
672   https://doi.org/10.1007/s10980-012-9826-0

673

Supplements

Table of Contents

S1. Model output and additional results

Temporal patterns in drought magnitude

Table S1. ANOVA results for linear models testing short- and long-term temporal trends in drought magnitude. We tested for the effect of year and year squared on drought magnitude (i.e. cumulative climatic water balance in mm from May-Aug each year, see main text). We report model estimates with standard errors (SE) the sum of squares (SumSq) and mean squares (MeanSq), degrees of freedom (DF), F-value, and P-value (P<0.10 in bold). As there was no support for a nonlinear trend on the short-term, we dropped year squared from the final model for 2000-2023.

Model parameter	Estimate (SE)	SumSq/MeanSq	DF	F-value	P-value
Short-term (2000-2023) – full					
Year	1,238.79 (1,344.00)	17,338.18/17,338.18	1	3.54	**0.07**
Year^2	-0.31 (0.33)	4,184.26/4,184.26	1	0.85	0.37
Residuals		102,782.79/4894.42	21		
Short-term (2000-2023) – reduced					
Year	-3.88 (2.06)	17,338.18/17,338.18	1	3.57	**0.07**
Residuals		106,967.04/4,862.14	22		
Long-term (1959-2023)					
Year	191.89 (107.26)	4,895.85/4,895.85	1	1.05	0.31
Year^2	-0.05 (0.03)	15,023.10/15,023.10	1	3.22	**0.08**
Residuals		289,636.21/4,671.55	62		
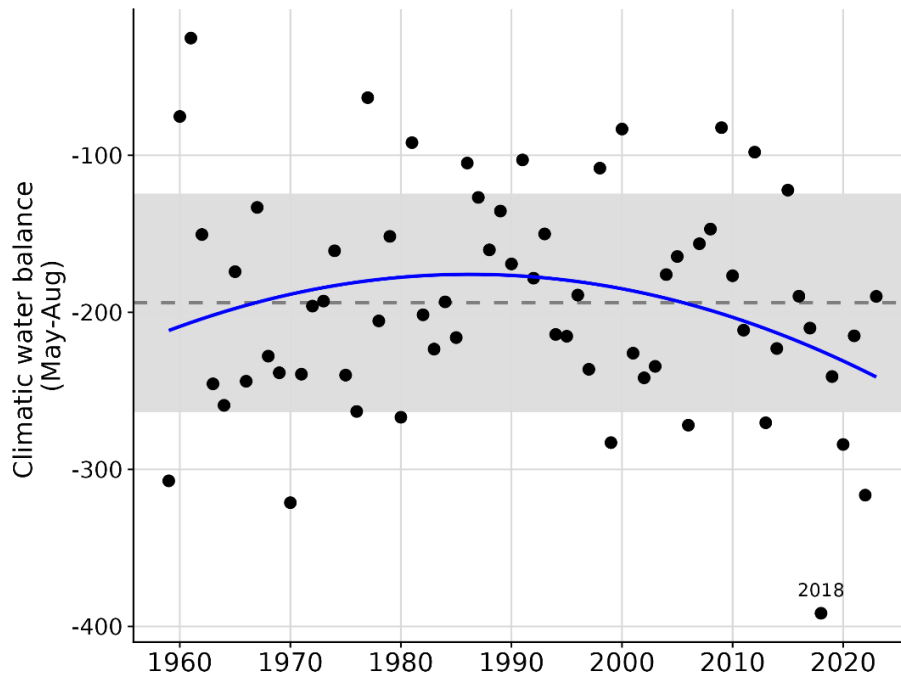
Fig S1. Nonlinear long-term trend in drought magnitude on the Åland islands, Finland. Drought magnitude per year (black points) for the time period 1959-2023 was measured as cumulative climatic water balance during the butterfly's growing season (May-Aug, see Methods). The grey dashed line and shaded area give the long-term average ± 1 standard deviation (std.dev) and the blue line gives the long-term trend in drought magnitude (Table S1). Note that 2018 is the driest year on record, and no wetter than average years (>1 std.dev of the mean) were observed in the last 8 years.

Landsat model coefficients

Table S2. Model coefficients for the full occupancy and abundance models using Landsat satellite data (2000-2023). The full model included five covariates known to majorly contribute to *Melitaea cinxia* metapopulation dynamics (i.e. patch habitat area, population connectivity, host plant abundance, patch population size in the previous year, and grazing intensity; see main text), as well as fixed effects capturing between-patch and within-patch vegetation heterogeneity estimated using Normalized Difference Vegetation Indices (NDVI) per patch – the mean NDVI, mean squared (mean^2), and standard deviation (sd), and their interactions with host plant abundance. Posterior means, sd, and 95% Credible Intervals (CI) are given, with 95% CIs that did not overlap with zero in bold (i.e. P<0.05).

Fixed effect	Posterior mean	Posterior sd	95% CI		
occupancy					
intercept	-2.92	0.23	**-3.37**	**–**	**-2.47**
area	0.32	0.02	**0.28**	**–**	**0.37**
connectivity	0.84	0.02	**0.80**	**–**	**0.88**
grazing intensity	-0.28	0.02	**-0.31**	**–**	**-0.24**
hostplant	0.92	0.03	**0.87**	**–**	**0.97**
previous popsize	0.50	0.01	**0.48**	**–**	**0.53**
NDVI_mean	-0.28	0.03	**-0.35**	**–**	**-0.21**
NDVI_mean^2	-0.11	0.02	**-0.15**	**–**	**-0.08**
NDVI_sd	-0.05	0.03	-0.10	–	0.01
hostplant:NDVI_mean	0.12	0.03	**0.06**	**–**	**0.19**
hostplant:NDVI_mean^2	0.01	0.02	-0.03	–	0.04
hostplant:NDVI_sd	-0.05	0.03	-0.10	–	0.005
abundance					
intercept	-0.47	0.13	**-0.73**	**–**	**-0.21**
area	0.28	0.02	**0.24**	**–**	**0.33**
connectivity	0.22	0.02	**0.19**	**–**	**0.25**
grazing intensity	-0.06	0.02	**-0.10**	**–**	**-0.02**
hostplant	0.32	0.03	**0.26**	**–**	**0.38**
previous popsize	0.26	0.01	**0.24**	**–**	**0.28**
NDVI_mean	-0.04	0.04	-0.12	–	0.03
NDVI_mean^2	-0.06	0.02	**-0.10**	**–**	**-0.01**
NDVI_sd	-0.04	0.04	-0.12	–	0.03
hostplant:NDVI_mean	0.06	0.04	-0.02	–	0.13
hostplant:NDVI_mean^2	0.02	0.02	-0.03	–	0.07
hostplant:NDVI_sd	-0.02	0.04	-0.10	–	0.06
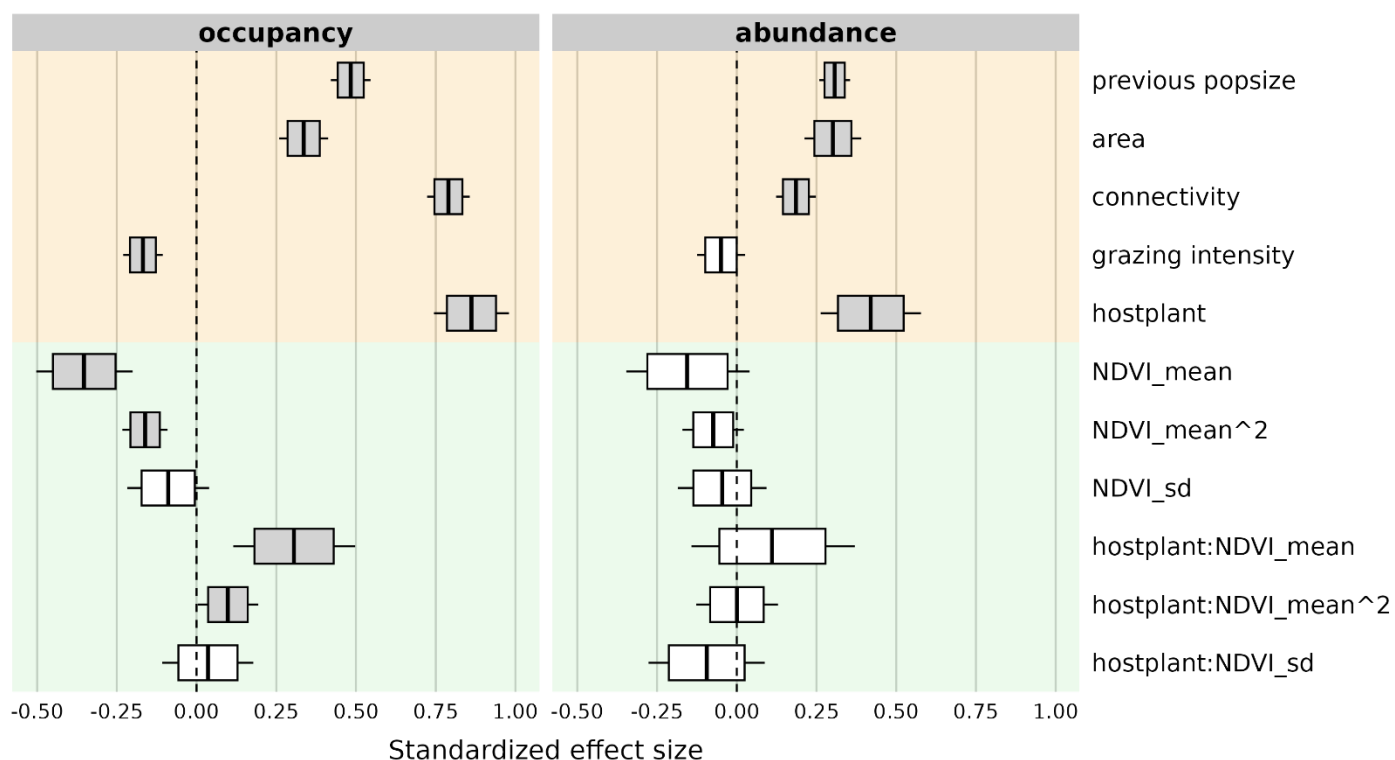
41   **Figure S2. Standardized effect sizes of vegetation productivity and heterogeneity on**
42   **butterfly patch occupancy and abundance dynamics (2016-2023).** Both the
43   occupancy and abundance models contained five fixed effects previously found to
44   influence *M. cinxia* metapopulation dynamics (i.e. covariates highlighted in orange:
45   population size in the previous year, patch area, connectivity, grazing intensity, and host
46   plant abundances) as well as fixed effects capturing between-patch and within-patch
47   vegetation heterogeneity (highlighted in green), as estimated from Sentinel satellite data
48   by the mean Normalized Difference Vegetation Index (NDVI), mean NDVI squared and
49   NDVI standard deviation (sd) per patch (see Methods). For each fixed effect the posterior
50   means are shown with boxes depicting the 80% Credible Intervals [CI] and whiskers the
51   95% CIs, colored grey when the 95% CIs did not overlap with zero (i.e. P<0.05, Table S3).

Table S3. Model coefficients for the full occupancy and abundance models using
Sentinel satellite data (2016-2023). Posterior means, sd, and 95% Credible Intervals
(CI) are given for included covariates (patch habitat area, population connectivity, host
plant abundance, patch population size in the previous year, and grazing intensity) and
fixed effects (Normalized Difference Vegetation Indices [NDVI] per patch); with 95% CIs
that did not overlap with zero in bold (i.e. P<0.05). See Fig.2 and Table S2 for model results
using Landsat satellite data (2000-2023).

Fixed effect	Posterior mean	Posterior SD	95% CI		
occupancy					
intercept	-2.97	0.56	**-4.06**	**–**	**-1.88**
area	0.34	0.04	**0.26**	**–**	**0.41**
connectivity	0.79	0.03	**0.72**	**–**	**0.86**
grazing intensity	-0.17	0.03	**-0.23**	**–**	**-0.11**
hostplant	0.86	0.06	**0.74**	**–**	**0.98**
previous popsize	0.48	0.03	**0.42**	**–**	**0.55**
NDVI_mean	-0.35	0.08	**-0.50**	**–**	**-0.20**
NDVI_mean^2	-0.16	0.04	**-0.23**	**–**	**-0.09**
NDVI_sd	-0.09	0.07	-0.22	–	0.04
hostplant:NDVI_mean	0.31	0.10	**0.12**	**–**	**0.50**
hostplant:NDVI_mean^2	0.10	0.05	**0.003**	**–**	**0.19**
hostplant:NDVI_sd	0.04	0.07	-0.11	–	0.18
abundance					
intercept	-0.58	0.30	-1.18	–	0.02
area	0.30	0.05	**0.21**	**–**	**0.39**
connectivity	0.19	0.03	**0.12**	**–**	**0.25**
grazing intensity	-0.05	0.04	-0.13	–	0.03
hostplant	0.42	0.08	**0.26**	**–**	**0.58**
previous popsize	0.31	0.02	**0.26**	**–**	**0.36**
NDVI_mean	-0.16	0.10	-0.35	–	0.04
NDVI_mean^2	-0.07	0.05	-0.17	–	0.02
NDVI_sd	-0.05	0.07	-0.18	–	0.09
hostplant:NDVI_mean	0.11	0.13	-0.14	–	0.37
hostplant:NDVI_mean^2	0.001	0.07	-0.13	–	0.13
hostplant:NDVI_sd	-0.09	0.09	-0.28	–	0.09

59

Effect size modulation by drought model output
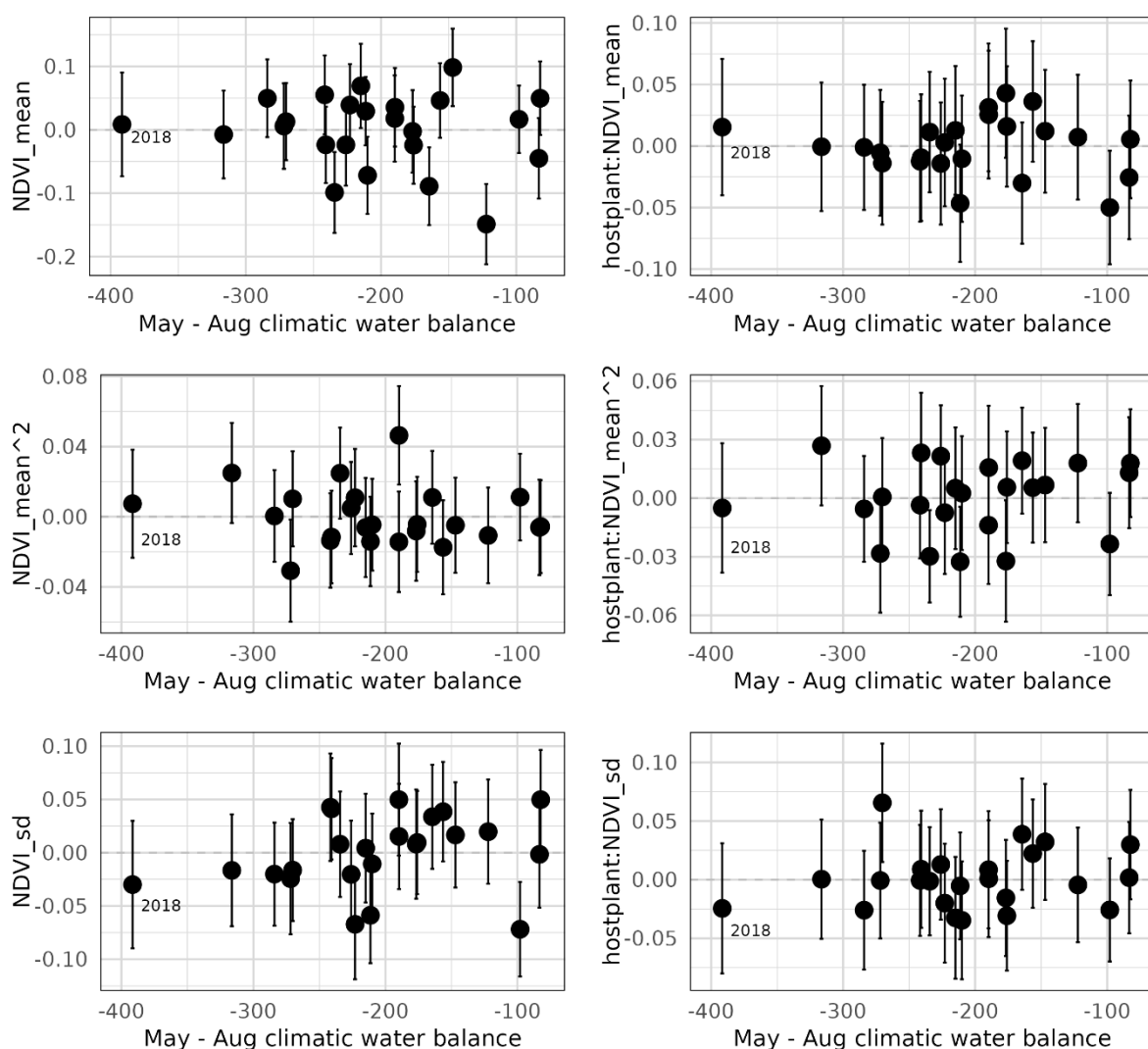
Figure S4. No drought magnitude modulation of vegetation productivity and heterogeneity effect sizes on butterfly occupancy dynamics. Each panel shows the relationship between drought magnitude on the x-axis (measured as the cumulative climatic water balance in mm during the butterfly growing season May-Aug) and on the y-axis the yearly slope effect sizes of each Normalized Difference Vegetation Index (NDVI) fixed effect and their interactions with host plant abundance on patch occupancy (see Fig.2 and Table S2 for the fixed effect model coefficients). Points are the posterior mean year slope effect sizes ± posterior standard deviation. No significant trends of drought magnitude and/or drought magnitude squared on NDVI effect sizes were found (P>0.10, Table S5).

Table S5. ANOVA results for linear models testing whether drought magnitude impacts the effect size of vegetation heterogeneity on occupancy dynamics. We tested for the effect of drought magnitude (WAB58) and drought magnitude squared (WAB58^2), measured as cumulative climatic water balance during the butterfly's growing season (May-Aug). Drought magnitude squared was dropped from the final model when not significant (P>0.10). Annual random effect sizes (i.e. posterior means) of each vegetation heterogeneity fixed effect and their interaction effects were obtained from the full occupancy model (Fig. 2 and Table S2). For each fixed effect, we ran a simple linear model as well as a more complex linear model that took into account the estimation error around the vegetation heterogeneity effect sizes (i.e. ± posterior standard deviation). Estimates are given for the simple linear models, including the degrees of freedom (DF) and residual DF, F-value and p-value, reported for models including and excluding the year of the extreme event 2018. For the more complex Bayesian models we only included the 90% Credible Intervals (CI) here, as in all cases the estimates were in the same direction and of similar magnitude as the simple linear models. No effects of drought magnitude on vegetation heterogeneity effect sizes were observed (also see Fig.S4).

Fixed effect	Estimate (excl. 2018)	90% CI			DF (resDF)	F-value	P-value (excl. 2018)
NDVI_mean							
WAB58	-0.01 (-0.01)	-0.03	–	0.02	1 (21)	0.24	0.63 (0.64)
WAB58^2	<-0.001 (<0.001)	-0.02	–	0.02	1 (21)	0.01	0.94 (0.94)
reduced model:							
WAB58	-0.01 (-0.01)				1 (22)	0.25	0.62 (0.63)
NDVI_mean^2							
WAB58	-0.002 (-0.002)	-0.01	–	0.01	1 (21)	0.54	0.47 (0.57)
WAB58^2	<0.001 (0.001)	-0.01	–	0.01	1 (21)	0.09	0.76 (0.66)
reduced model:							
WAB58	-0.003 (-0.002)				1 (22)	0.56	0.46 (0.56)
NDVI_sd							
WAB58	0.01 (0.01)	-0.01	–	0.03	1 (21)	1.68	0.21 (0.35)
WAB58^2	-0.003 (-0.005)	-0.02	–	0.01	1 (21)	0.36	0.55 (0.47)
reduced model:							
WAB58	0.01 (0.01)				1 (22)	1.73	0.20 (0.34)
hostplant:NDVI_mean							
WAB58	-0.003 (<0.001)	-0.02	–	0.02	1 (21)	0.21	0.65 (0.90)
WAB58^2	-0.001 (-0.006)	-0.01	–	0.01	1 (21)	0.16	0.69 (0.18)
reduced model:							

7

Fixed effect	Estimate (excl. 2018)	90% CI			DF (resDF)	F-value	P-value (excl. 2018)
WAB58	-0.002 (<-0.001)				1 (22)	0.21	0.65 (0.90)
hostplant:NDVI_mean^2							
WAB58	0.003 (0.001)	-0.01	–	0.01	1 (21)	0.30	0.59 (0.64)
WAB58^2	0.002 (0.004)	-0.01	–	0.01	1 (21)	0.44	0.52 (0.29)
reduced model:							
WAB58	0.002 (0.002)				1 (22)	0.31	0.58 (0.64)
hostplant:NDVI_sd							
WAB58	0.004 (<0.001)	-0.01	–	0.02	1 (21)	0.56	0.46 (0.80)
WAB58^2	<-0.001 (0.003)	-0.01	–	0.01	1 (21)	0.05	0.82 (0.59)
reduced model:							
WAB58	0.004 (0.001)				1 (22)	0.58	0.45 (0.79)

Table S6. ANOVA results for linear models testing whether drought magnitude impacts the effect size of vegetation heterogeneity on abundance dynamics. We report the effects of drought magnitude (WAB58), and drought magnitude squared (WAB58^2) on each vegetation heterogeneity fixed effect included in the full abundance model (see Fig. 2 and Table S2). Drought magnitude squared was dropped from the final model when not significant (P>0.10). Estimates are given for the simple linear models (see Table S5 legend for details), including the degrees of freedom (DF) and residual DF, F-value and p-value, reported for models including and excluding the year of the extreme event 2018. For the more complex Bayesian models we only included the 90% Credible Intervals (CI) here, as in all cases the estimates were in the same direction and of similar magnitude as the simple linear models. Significant trends are in bold (P<0.10), with robust results highlighted in grey (i.e. cases where drought magnitude was significant both in the simple and more complex linear models).

Fixed effect	Estimate (excl. 2018)	90% CI			DF (resDF)	F-value	P-value (excl. 2018)
NDVI_mean							
WAB58	-0.02 (-0.02)	-0.04	–	0.004	1 (21)	6.42	**0.02 (0.02)**
WAB58^2	-0.004 (-0.002)	-0.02	–	0.01	1 (21)	0.71	0.41 (0.74)
reduced model:							
WAB58	-0.02 (-0.02)				1 (22)	6.50	**0.02 (0.02)**
NDVI_mean^2							
WAB58	-0.002 (-0.004)	-0.02	–	0.01	1 (21)	0.08	0.78 (0.47)
WAB58^2	-0.003 (<0.001)	-0.01	–	0.01	1 (21)	0.50	0.49 (0.92)
reduced model:							
WAB58	-0.002 (-0.004)				1 (22)	0.08	0.78 (0.46)

8

NDVI_sd

WAB58	0.02 (0.02)	**0.003**	**–**	**0.05**	1 (21)	4.44	**0.05 (0.03)**
WAB58^2	0.01 (0.01)	-0.01	–	0.03	1 (21)	2.47	0.13 (0.30)
reduced model:							
WAB58	0.02 (0.02)				1 (22)	4.16	**0.05 (0.03)**

hostplant:NDVI_mean

WAB58	-0.01 (-0.01)	-0.03	–	0.01	1 (21)	3.23	**0.09** *(0.13)*
WAB58^2	<0.001 (0.002)	-0.01	–	0.01	1 (21)	0.004	0.95 (0.75)
reduced model:							
WAB58	-0.01 (-0.01)				1 (22)	3.39	**0.08** *(0.13)*

hostplant:NDVI_mean^2

WAB58	0.003 (0.002)	-0.01	–	0.02	1 (21)	0.47	0.50 (0.81)
WAB58^2	-0.003 (-0.002)	-0.01	–	0.01	1 (21)	0.44	0.51 (0.77)
reduced model:							
WAB58	0.004 (0.002)				1 (22)	0.48	
							0.50 (0.80)

hostplant:NDVI_sd

WAB58	0.03 (0.02)	-0.01	–	0.06	1 (21)	2.59	0.12 (0.14)
WAB58^2	0.02 (0.03)	-0.01	–	0.04	1 (21)	1.87	0.19 *(0.06)*
reduced model:							
WAB58	0.03 (NA)				1 (22)	2.49	0.13 (NA)

103